Organic & Biomolecular Chemistry

ROYAL SOCIETY OF CHEMISTRY

COMMUNICATION

View Article Online
View Journal | View Issue

Cite this: *Org. Biomol. Chem.*, 2025, **23**, 4888

Received 17th March 2025,
Accepted 14th April 2025

DOI: 10.1039/d5ob00587f

rsc.li/obc

Asymmetric synthesis of C–N axially chiral carbazoles *via* axial-to-axial chirality transfer†

Sebastian Myllek, [a] Philip Lencer,[b] Moritz K. T. Klischan, [a] Birgit Henssen,[b] Philipp Neudecker, [c,d] Martin Breugst *[e] and Jörg Pietruszka *[a,b]

C–N axially chiral carbazole derivatives were synthesised by an intramolecular Buchwald–Hartwig amination starting from C–C axially chiral biaryls utilising an axial-to-axial chirality transfer with enantiospecificities up to 91%. The mechanism of the chirality transfer was investigated *via* DFT calculations.

Axially chiral, *N*-arylated carbazoles are intriguing structural motifs that occur in natural products, chiral organocatalysts and phosphine ligands (Scheme 1a).[1] So far, only a limited number of racemic and atroposelective syntheses have been reported in the literature, showcasing the relative scarcity of synthetic methods for this type of stereogenic C–N bond.[2] Building on early reports on the synthesis of C–N axially chiral anilids *via* inter- or intramolecular Buchwald–Hartwig aminations, the development of atroposelective synthesis methods for C–N axially chiral biaryls has only recently gained momentum.[3] Most of these methods follow one of three approaches: (I) *de novo* ring construction, (II) stereoselective functionalisation of C–N-linked biaryls or (III) direct formation of the stereogenic bond *via* aryl amination. Strategies following the first approach typically start from non-biaryl structures such as diarylamine precursors, which were successfully annulated *via* transition metal or Brønsted acid catalysis.[4] The second approach focuses on establishing chirality *via* atroposelective *ortho*-functionalisation of achiral biaryls, while kinetic resolution and desymmetrisation were also reported.[5] Other contributions include Rh-catalysed cycloadditions to alkynyl indoles and annulation of sulfoxonium ylides.[6] The third concept consolidates C–N bond formation and establishment of axial chirality into a single step. Chiral Brønsted acids served as efficient catalysts for the asymmetric amination of azonaphthalenes and indolinone derivatives, while *N*-aryl-indolines and indolocarbazoles were accessed *via* transition metal catalysis.[1a,2d,7] Recently, a C–C to C–N axial-to-axial chirality transfer was developed by Liu *et al.* in a Catellani-type reaction for the synthesis of C–N axially chiral phenanthridinones and later extended to other heterocycles.[8] In this work, we have expanded the concept of axial-to-axial chirality transfer and developed an atroposelective synthesis of C–N axially chiral carbazoles starting from C–C axially chiral biaryls (Scheme 1b). Separating the formation of the C–C stereogenic bond and the chirality transfer into different reactions allowed us to elucidate the underlying principles and investigate the mechanism *via* DFT calculations.

We started our investigations by computing the rotational barriers of different *N*-arylated carbazoles *via* DFT, identifying

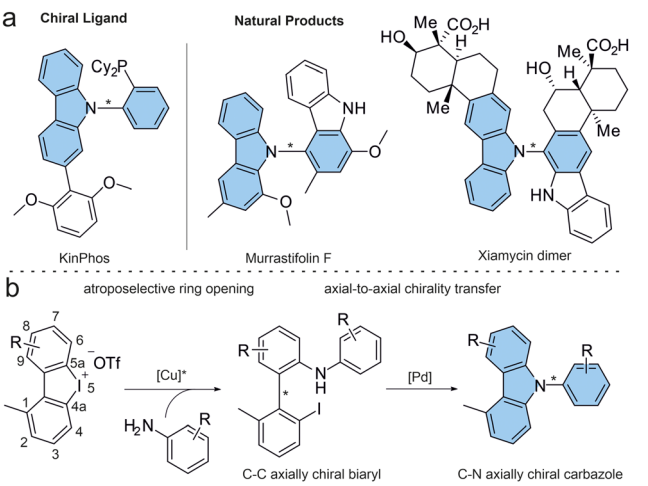

Scheme 1 a) Axially chiral carbazoles; (b) axial-to-axial chirality transfer in carbazole synthesis.

[a]*Institut für Bioorganische Chemie, Heinrich-Heine-Universität Düsseldorf im Forschungszentrum Jülich, Stetternicher Forst, 52426 Jülich, Germany. E-mail: j.pietruszka@fz-juelich.de*
[b]*Institut für Bio- und Geowissenschaften (IBG-1: Bioorganische Chemie), Forschungszentrum Jülich GmbH, Wilhelm-Johnen Straße, 52428 Jülich, Germany*
[c]*Institut für Physikalische Biologie, Heinrich-Heine-Universität Düsseldorf, 40225 Düsseldorf, Germany*
[d]*IBI-7 – Strukturbiochemie, Forschungszentrum Jülich, 52425 Jülich, Germany*
[e]*Institut für Chemie, Technische Universität Chemnitz, Straße der Nationen 62, 09111 Chemnitz, Germany. E-mail: martin.breugst@chemie.tu-chemnitz.de*
†Electronic supplementary information (ESI) available. See DOI: https://doi.org/10.1039/d5ob00587f

carbazoles **4**, **5** and **8** as suitable chiral targets. With rotational barriers between 32 and 36 kcal mol^{-1}, all carbazoles exceed the necessary barrier of 22.3 kcal mol^{-1} and have isomerisation half-lives of many years (Scheme 2).[9] Interestingly, carbazole **8** showed a higher barrier than 1-methyl substituted derivatives **4** and **5**. This can be attributed to a destabilised ground state due to repulsion between the C-1 methyl group and the *N*-aryl substituent, an effect previously described in the literature.[8a,10]

Our synthetic strategy was based on a divergent approach utilising the copper-catalysed ring opening of strained iodonium salts as a branching point (Scheme 2).[11] To utilise this route for the synthesis of C–N axially chiral carbazoles, the corresponding iodonium salt must not be C_2-symmetric. Consequently, two regioisomers can result from the ring opening taking place at carbon C-4a or C-5a, respectively. Iodonium salt **1** was chosen as the first synthetic target, with the aim to sterically direct the ring opening towards carbon 5a *via* the C-4 substituent (Scheme 2). **1** was accessed in 59% total yield over 4 steps from commercial starting materials, as described by Zhao *et al.* (for full details, refer to the ESI†).[11] Due to the sterically challenging nature of the ring opening of **1** using *ortho*-substituted anilines, a catalytic, enantioselective reaction was not successful.[12] However, under high catalyst loadings of *rac*-BINAP-Cu(OAc)$_2$, racemic biaryls **2** and **3** could be isolated in moderate to good yields and subsequently resolved using preparative chiral HPLC. Notably, in both cases, only one regioisomer was obtained. Subsequent intramolecular cyclisation under standard Buchwald–Hartwig conditions produced carbazoles **4** and **5** with 71% ee and 40% ee, respectively (Scheme 2).

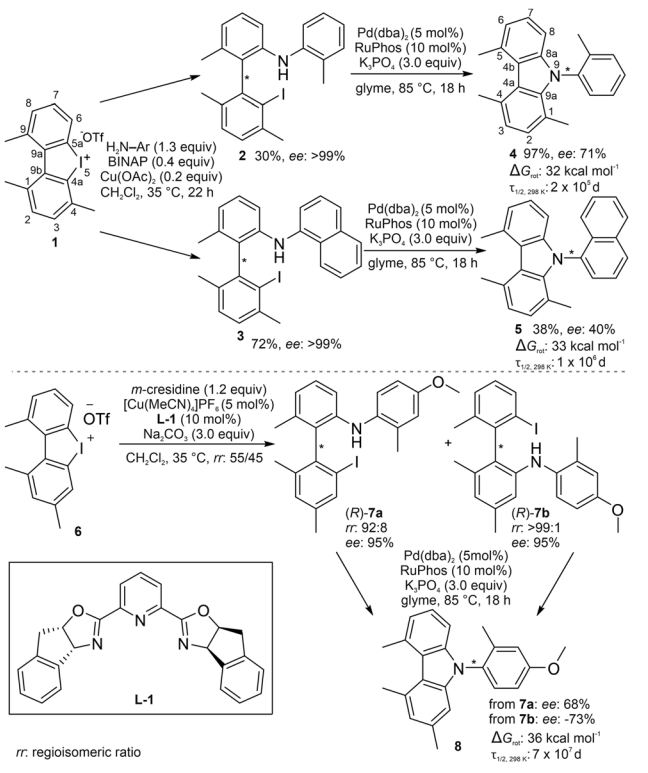

Scheme 2 Synthesis of carbazoles **4**, **5** and **8** starting from iodonium salts **1** and **6** *via* C–C axially chiral biaryls **2**, **3** and **7**. ΔG_{rot}: computed rotational barrier (ωB97M-V/def2-TZVPP//r^{2}SCAN-3c);[13] $\tau_{1/2,\ 298\ K}$: half-life at 298 K.

Having demonstrated the viability of the chirality transfer, we directed our efforts towards the asymmetric construction of the key biaryls. To minimize steric hindrance in the ring opening reaction, iodonium salt **6** was chosen as an alternative branching point. [Cu(MeCN)$_4$]PF$_6$ in combination with PyBox-ligand **L-1** was a suitable catalyst for the enantioselective ring opening, however, with low regioselectivity. Regioisomers **7a** and **7b** were obtained with 95% ee each, in a ratio of 55 : 45. *m*-Cresidine was used instead of *o*-toluidine to facilitate separation of the regioisomers using preparative HPLC. Cyclisation of **7a** and **7b** to carbazole **8** proceeded with similar efficiencies, but opposite selectivities in the chirality transfer. While **7a** afforded (+)-**8** with 68% ee, **7b** yielded (−)-**8** with 73% ee (Scheme 2). To assess whether the inverse enantioselectivity is a result of intrinsic enantiocomplementarity or if the regioisomers themselves are formed with opposite absolute configuration during the ring opening of **6**, we assigned the absolute configuration of **7a** and **7b** *via* CD spectroscopy. In both cases, the experimental CD spectrum showed good agreement with the computed spectra for (*R*)-**7a** and (*R*)-**7b**, which were obtained from TD-DFT calculations. As most biaryl precursors used in this study were not enantiopure (>99% ee), enantiospecificity (es) is used as a comparable measure to express the efficiency of the chirality transfer: es = ($ee_{product}/ee_{starting\ material}$) × 100%.[14] For the synthesis of **8** starting from **7a** and **7b**, enantiospecificities of 72% and 77% are calculated. Correcting for the lower regioisomeric ratio of **7a** compared to **7b** (92 : 8 *vs.* >99 : 1) an enantiospecificity of 81% is predicted for pure **7a**, indicating small quantitative differences in the enantiospecificity, besides the previously discussed inverse selectivity.

We next proceeded with a screening of the intramolecular Buchwald–Hartwig amination. Due to the inverse enantioselectivity, facile separation of the biaryl regioisomers was required. Ring opening of chlorinated iodonium salt **9** yielded regioisomers **10a** and **10b** in a 59 : 41 ratio, which were separable *via* column chromatography (Scheme 3a) (for complete screening, see the ESI†). Starting with our initial catalyst system RuPhos-Pd(dba)$_2$, a temperature screening from 65 °C to 85 °C showed only marginal effects on the es, while the yield deteriorated below 65 °C (Scheme 3b; entries 1–3). In contrast, the ligands had a much more pronounced effect on the es, and a positive correlation of enantiospecificity with steric bulk as well as an inverse correlation with electron richness was observed (entries 4–10). While electron-rich PCy$_3$ produced only a marginal es of 9% (entry 4), P(4-CF$_3$C$_6$H$_4$)$_3$ was the best performing ligand with 88% es (entry 6). Buchwald-type and chelating ligands generally performed robustly in terms of yield and es. Interestingly, employing enantiopure chiral ligands had no effect on the es compared to the racemic ligand, and no matched or mismatched cases were observed

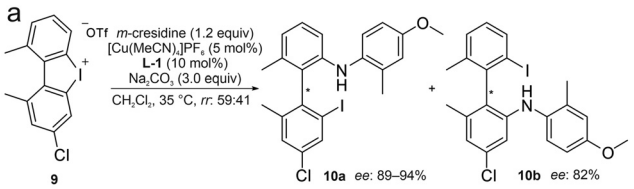

#	ligand	temperature [°C]	solvent	base	conv.[a] [%]	es[b] [%]
1	RuPhos	85	Glyme	K_3PO_4	72	82
2	RuPhos	75	Glyme	K_3PO_4	69	85
3	RuPhos	65	Glyme	K_3PO_4	51	83
4	PCy_3	85	Glyme	K_3PO_4	65	9
5	PPh_3	85	Glyme	K_3PO_4	60	41
6	$P(4\text{-}CF_3C_6H_4)_3$	85	Glyme	K_3PO_4	82	88
7	*rac*-BINAP	85	Glyme	K_3PO_4	56	85
8	(*R*)-BINAP	85	Glyme	K_3PO_4	77	87
9	(S)-BINAP	85	Glyme	K_3PO_4	87	87
10	*i*Pr-NHC	85	Glyme	K_3PO_4	26	63
11	$P(4\text{-}CF_3C_6H_4)_3$	65	Glyme	*t*-BuOK	84	90
12	$P(4\text{-}CF_3C_6H_4)_3$	65	toluene	*t*-BuOK	96	14
13	$P(4\text{-}CF_3C_6H_4)_3$	65	1,4-dioxane	*t*-BuOK	45	54
14	$P(4\text{-}CF_3C_6H_4)_3$	65	DMF	*t*-BuOK	96	88

Scheme 3 a) Synthesis and resolution of substrates **10a** and **10b**; (b) screening conditions. [a] Conversion to product determined *via* ^{1}H-NMR. [b] Enantiospecificity; for ee values, see the ESI.†

(entries 7–9). The iPr-NHC ligand did not perform well in the reaction (entry 10). Switching the base to *t*-BuOK showed a small positive effect on yield and es (entry 11). In contrast, solvents had a pronounced influence, with toluene and 1,4-dioxane producing only 14% es and 54% es, respectively. DMF performed well, with 88% es (entries 12–14). Concluding the screening, we applied the optimized conditions to the syntheses of carbazoles **4**, **5** and **8**. While carbazoles **4** and **5** were synthesized with increased es of 84% (previously 71%) and 62% (previously 40%), respectively, **8** was formed with a lower es of 63% (previously 77%).

We next investigated the relationship between the structure of the biaryls and enantiospecificity of the cyclisation by synthesizing additional carbazole derivatives. As a logical extension to 4-chloro substituted **10a**, the 4-fluoro derivative produced the corresponding carbazole **12** with a similar 86% es (Scheme 4). A fruitful approach was the introduction of a tosylate at position R^1, which greatly facilitated the chromatographic separation of the corresponding biaryl regioisomers. Furthermore, cyclisation towards carbazole **13** showed the highest chirality transfer efficiency of 91%. Probing the effect of sterically demanding *N*-aryl substituents, 2′-ethyl and 2′-isopropyl substituted carbazoles **14** and **15** were accessed with reduced enantiospecificities of 44% es and 56% es, respectively. Concluding our synthetic studies, we explored the mechanism of the chirality transfer *via* DFT calculations. A plausible pathway is depicted in Scheme 5, following the generally accepted catalytic cycle of the Buchwald–Hartwig amination *via* oxidative addition, amine coordination, deprotonation, ligand exchange and reductive elimination.[15] Our investi-

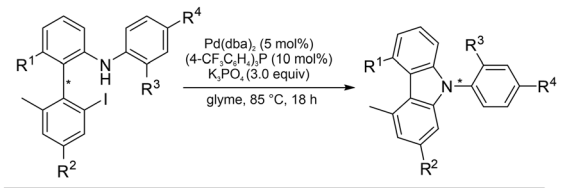

#	R^1	R^2	R^3	R^4	yield [%]	es [%]
12	Me	F	Me	OMe	83	86
13	OTs	H	Me	OMe	92	91
14	OTs	H	Et	H	91	44
15	OTs	H	*i*-Pr	H	86	56

Scheme 4 Scope of carbazole synthesis. es: enantiospecificity; for ee values, see the ESI.†

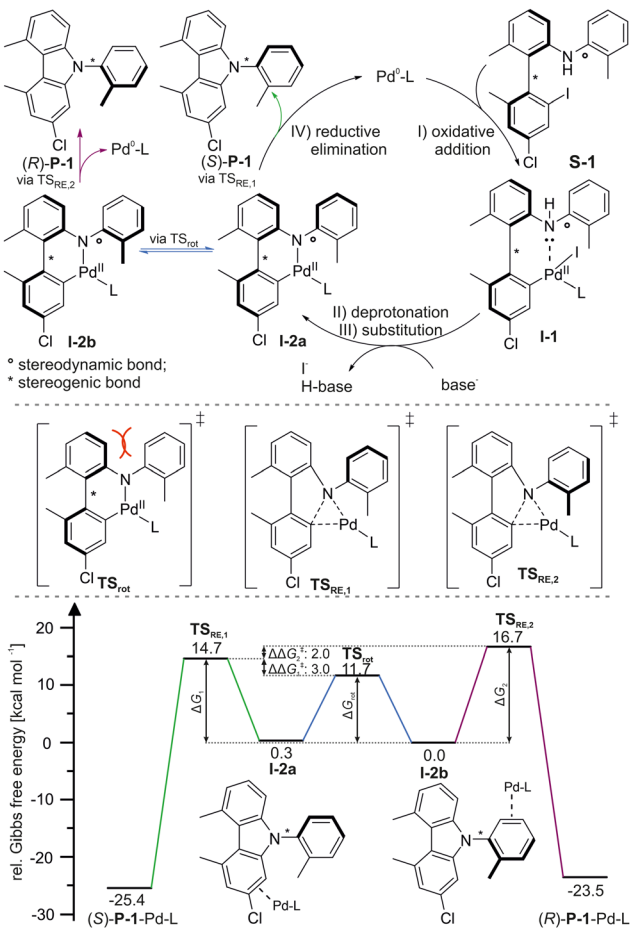

Scheme 5 Plausible mechanistic pathway of the cyclisation and energy profile of the reductive elimination (ωB97M-V/def2-TZVPP/SMD(DMF)//TPSS-D4/def2-SVP).[16]

gations were based on two hypotheses: (1) the reaction proceeds *via* two diastereomeric intermediates (Scheme 5: **I-2a**/**I-2b**), which form one or the other carbazole enantiomer. (2) These two intermediates interconvert *via* a C–N bond rotation (marked with °). If the interconversion of the intermediates (*via* $\mathbf{TS_{rot}}$) is fast compared to carbazole formation, the chirality transfer proceeds under Curtin–Hammett conditions and the enantioselectivity is determined by the $\Delta\Delta G^{\ddagger}$ of the corresponding transition states $\mathbf{TS_{RE,1}}$ and $\mathbf{TS_{RE,2}}$. Conformational analysis revealed intermediates **I-2a** and **I-2b**, with **I-2a** being slightly disfavoured by 0.3 kcal mol^{-1}. $\mathbf{TS_{rot}}$ was located at a dihedral angle of 3.3°, and a $\Delta G^{\ddagger}$ of 11.7 kcal mol^{-1} was calculated with respect to **I-2b**. Two transition states were identified for reductive elimination. Starting from **I-2a**, $\mathbf{TS_{RE,1}}$ was located at a relative Gibbs energy of 14.7 kcal mol^{-1}, while the corresponding $\mathbf{TS_{RE,2}}$ – starting from **I-2b** – had a higher energy of 16.7 kcal mol^{-1}. From a $\Delta\Delta G_1^{\ddagger}$ of 3.0 kcal mol^{-1}, it follows that the interconversion of **I-2a** and **I-2b** is more than 100-fold faster than the reductive elimination, indicating Curtin–Hammett conditions. The (*S*)-configuration is predicted for the main product, with an enatiomeric ratio (er) of 97 : 3, matching the experimental absolute configuration of (*S*)-**11** determined by CD spectroscopy (see the ESI†). The predicted er is in good agreement with the experimental distribution of 95 : 5 of (*S*)-**11** (assuming 90% es and enantiopure starting material).

Data availability

The data supporting this article have been included as part of the ESI.†

Conflicts of interest

There are no conflicts to declare.

Acknowledgements

We gratefully acknowledge the Studienstiftung des deutschen Volkes e. V., the Heinrich Heine University Düsseldorf, the Forschungszentrum Jülich GmbH, the DFG (GRK2158 and BR 5154/4-1) and the Technische Universität Chemnitz for their continued support.

References

1 (*a*) W. Xia, Q.-J. An, S.-H. Xiang, S. Li, Y.-B. Wang and B. Tan, *Angew. Chem., Int. Ed.*, 2020, **59**, 6775–6779; (*b*) K. B. Gan, R.-L. Zhong, Z.-W. Zhang and F. Y. Kwong, *J. Am. Chem. Soc.*, 2022, **144**, 14864–14873; (*c*) C. Ito, Y. Thoyama, M. Omura, I. Kajiura and H. Furukawa, *Chem. Pharm. Bull.*, 1993, **41**, 2096–2100; (*d*) Z. Xu, M. Baunach, L. Ding and C. Hertweck, *Angew. Chem., Int. Ed.*, 2012, **51**, 10293–10297.

2 (*a*) G. Bringmann, S. Tasler, H. Endress, J. Kraus, K. Messer, M. Wohlfarth and W. Lobin, *J. Am. Chem. Soc.*, 2001, **123**, 2703–2711; (*b*) C. Börger, A. W. Schmidt and H.-J. Knölker, *Synlett*, 2014, 1381–1384; (*c*) M. Zhang, P. Zhao, D. Wu, Z. Qiu, C. Zhao, W. Zhang, F. Li, J. Zhou and L. Liu, *J. Org. Chem.*, 2023, **88**, 2841–2850; (*d*) Q. Ren, T. Cao, C. He, M. Yang, H. Liu and L. Wang, *ACS Catal.*, 2021, **11**, 6135–6140.

3 (*a*) O. Kitagawa, M. Takahashi, M. Yoshikawa and T. Taguchi, *J. Am. Chem. Soc.*, 2005, **127**, 3676–3677; (*b*) O. Kitagawa, M. Yoshikawa, H. Tanabe, T. Morita, M. Takahashi, Y. Dobashi and T. Taguchi, *J. Am. Chem. Soc.*, 2006, **128**, 12923–12931; (*c*) T. Hirata, I. Takahashi, Y. Suzuki, H. Yoshida, H. Hasegawa and O. Kitagawa, *J. Org. Chem.*, 2016, **81**, 318–323.

4 (*a*) A. Arunachalampillai, P. Chandrappa, A. Cherney, R. Crockett, J. Doerfler, G. Johnson, V. C. Kommuri, A. Kyad, J. McManus, J. Murray, T. Myren, N. Fine Nathel, I. Ndukwe, A. Ortiz, M. Reed, H. Rui, M. V. Silva Elipe, J. Tedrow, S. Wells, S. Yacoob and K. Yamamoto, *Org. Lett.*, 2023, **25**, 5856–5861; (*b*) X. Wang, X.-J. Si, Y. Sun, Z. Wei, M. Xu, D. Yang, L. Shi, M.-P. Song and J.-L. Niu, *Org. Lett.*, 2023, **25**, 6240–6245; (*c*) G. Zhang, B. Yang, J. Yang and J. Zhang, *J. Am. Chem. Soc.*, 2024, **146**, 5493–5501; (*d*) P. Zhang, C.-Q. Guo, W. Yao, C.-J. Lu, Y. Li, R. S. Paton and R.-R. Liu, *ACS Catal.*, 2023, **13**, 7680–7690; (*e*) P. Zhang, X.-M. Wang, Q. Xu, C.-Q. Guo, P. Wang, C.-J. Lu and R.-R. Liu, *Angew. Chem., Int. Ed.*, 2021, **60**, 21718–21722.

5 (*a*) M. E. Diener, A. J. Metrano, S. Kusano and S. J. Miller, *J. Am. Chem. Soc.*, 2015, **137**, 12369–12377; (*b*) S. D. Vaidya, S. T. Toenjes, N. Yamamoto, S. M. Maddox and J. L. Gustafson, *J. Am. Chem. Soc.*, 2020, **142**, 2198–2203; (*c*) H. M. Snodgrass, D. Mondal and J. C. Lewis, *J. Am. Chem. Soc.*, 2022, **144**, 16676–16682; (*d*) Z.-J. Zhang, M. M. Simon, S. Yu, S.-W. Li, X. Chen, S. Cattani, X. Hong and L. Ackermann, *J. Am. Chem. Soc.*, 2024, **146**, 9172–9180; (*e*) J. Zhang, Q. Xu, J. Wu, J. Fan and M. Xie, *Org. Lett.*, 2019, **21**, 6361–6365; (*f*) U. Dhawa, T. Wdowik, X. Hou, B. Yuan, J. C. A. Oliveira and L. Ackermann, *Chem. Sci.*, 2021, **12**, 14182–14188; (*g*) L. Zhang, S.-H. Xiang, J. Wang, J. Xiao, J.-Q. Wang and B. Tan, *Nat. Commun.*, 2019, **10**, 566; (*h*) J. Wang, H. Chen, L. Kong, F. Wang, Y. Lan and X. Li, *ACS Catal.*, 2021, **11**, 9151–9158.

6 (*a*) P. Wang, H. Wu, X.-P. Zhang, G. Huang, R. H. Crabtree and X. Li, *J. Am. Chem. Soc.*, 2023, **145**, 8417–8429; (*b*) P. Wang, Y. Huang, J. Jing, F. Wang and X. Li, *Org. Lett.*, 2022, **24**, 2531–2535; (*c*) L. Zhou, Y. Li, S. Li, Z. Shi, X. Zhang, C.-H. Tung and Z. Xu, *Chem. Sci.*, 2023, **14**, 5182–5187; (*d*) X. Zhang, Q. Teng, Y. Ren, B. Wei, C.-H. Tung and Z. Xu, *Org. Chem. Front.*, 2024, **11**, 2857–2863.

7 (*a*) J. Frey, A. Malekafzali, I. Delso, S. Choppin, F. Colobert and J. Wencel-Delord, *Angew. Chem., Int. Ed.*, 2020, **59**, 8844–8848; (*b*) J. Rae, J. Frey, S. Jerhaoui, S. Choppin, J. Wencel-Delord and F. Colobert, *ACS Catal.*, 2018, **8**,

2805–2809; (*c*) C. Qian, J. Huang, T. Huang, L. Song, J. Sun and P. Li, *Chem. Sci.*, 2024, **15**, 3893–3900.

8 (*a*) Z.-S. Liu, P.-P. Xie, Y. Hua, C. Wu, Y. Ma, J. Chen, H.-G. Cheng, X. Hong and Q. Zhou, *Chem*, 2021, **7**, 1917–1932; (*b*) C. Wu, Z.-S. Liu, Y. Shang, C. Liu, S. Deng, H.-G. Cheng, H. Cong, Y. Jiao and Q. Zhou, *Chin. J. Chem.*, 2024, **42**, 699–704.

9 M. Ōki, in *Topics in Stereochemistry*, John Wiley & Sons Inc., 1983, pp. 1–81.

10 Y. Suzuki, I. Takahashi, Y. Dobashi, H. Hasegawa, C. Roussel and O. Kitagawa, *Tetrahedron Lett.*, 2015, **56**, 132–135.

11 K. Zhao, L. Duan, S. Xu, J. Jiang, Y. Fu and Z. Gu, *Chem*, 2018, **4**, 599–612.

12 X. Zhang, K. Zhao, N. Li, J. Yu, L.-Z. Gong and Z. Gu, *Angew. Chem., Int. Ed.*, 2020, **59**, 19899–19904.

13 (*a*) N. Mardirossian and M. Head-Gordon, *J. Chem. Phys.*, 2016, **144**, 214110; (*b*) F. Weigend and R. Ahlrichs, *Phys. Chem. Chem. Phys.*, 2005, **7**, 3297–3305; (*c*) S. Grimme, A. Hansen, S. Ehlert and J.-M. Mewes, *J. Chem. Phys.*, 2021, **154**, 064103; (*d*) F. Neese, *Wiley Interdiscip. Rev.: Comput. Mol. Sci.*, 2012, **2**, 73–78; (*e*) F. Neese, *Wiley Interdiscip. Rev.: Comput. Mol. Sci.*, 2022, **12**, e1606.

14 (*a*) D. Campolo, S. Gastaldi, C. Roussel, M. P. Bertrand and M. Nechab, *Chem. Soc. Rev.*, 2013, **42**, 8434–8466; (*b*) X.-L. Min, X.-L. Zhang, R. Shen, Q. Zhang and Y. He, *Org. Chem. Front.*, 2022, **9**, 2280–2292.

15 (*a*) J. F. Hartwig, *Synlett*, 1997, 329–340; (*b*) J. F. Hartwig, *Synlett*, 2006, 1283–1294.

16 (*a*) T. Yanai, D. P. Tew and N. C. Handy, *Chem. Phys. Lett.*, 2004, **393**, 51–57; (*b*) J. Tao, J. P. Perdew, V. N. Staroverov and G. E. Scuseria, *Phys. Rev. Lett.*, 2003, **91**, 146401; (*c*) A. V. Marenich, C. J. Cramer and D. G. Truhlar, *J. Phys. Chem. B*, 2009, **113**, 6378–6396; (*d*) E. Caldeweyher, C. Bannwarth and S. Grimme, *J. Chem. Phys.*, 2017, **147**, 034112.

